LAWRENCE
LIVERMORE
NATIONAL
LABORATORY

UCRL-JRNL-224169

Investigation of laser-induced damage in DKDP under multi-color irradiation

P. DeMange , R. A. Negres, A. M. Rubenchik, H. B. Radousky, M. D. Feit , S. G. Demos

September 5, 2006

Applied Physics Letters

Investigation of laser-induced damage in DKDP under multi-color irradiation

P. DeMange*, R. A. Negres, A. M. Rubenchik, H. B. Radousky*, M. D. Feit, and S. G. Demos

Lawrence Livermore National Laboratory, 7000 East Ave., Livermore, CA 94550

**and University of California, Davis Physics Department, 1 Shields Ave., Davis, CA 95616*

(Received

ABSTRACT

Laser-induced initiation of bulk damage sites in DKDP crystals is investigated under simultaneous exposure to 532- and 355-nm nanosecond laser pulses in order to simulate the operational conditions during harmonic conversion as well as probe the damage mechanisms. The results demonstrate synergetic damage effects under the dual-wavelength excitation. Furthermore, the damage performance is directly related to and can be predicted from the damage performance at each wavelength separately. The measured relative effective absorption coefficients at the two wavelengths are found to depend on the laser fluence.

Laser-induced damage sites initiated within the bulk of optical components is a key limiting factor in the development of high power laser systems. Potassium dihydrogen phosphate (KH_2PO_4 or KDP) and its deuterated analog ($KD_{2-x}H_xPO_4$ or DKDP) have been widely used for over three decades as Pockels cells and frequency converters and are still the only nonlinear materials suitable for large-aperture laser systems [1,2]. Damage thresholds in these materials have increased over time, primarily due to purer raw materials and improvement in growth processes, though localized damage sites still arise from laser intensities far below that necessary for intrinsic dielectric breakdown [3]. The damage precursors and their absorption mechanism leading to damage initiation are still unknown despite more than four decades of research [4,5]. In the case of KDP and DKDP crystals, recent work has highlighted the importance of synergetic effects between the second and third harmonics in Nd:glass lasers present during harmonic conversion to the observed damage density [6].

In this work, we quantitatively assess the damage performance of KDP/DKDP crystals under simultaneous exposure to the second and third harmonics of a nanosecond Nd:YAG laser system in order to a) probe the underlying mechanism of damage initiation and b) simulate the conditions taking place during harmonic conversion towards developing predictive models.

The experiments were made possible using a new damage testing approach where the density of damage sites (pinpoint density or PPD) formed in the bulk is directly measured. This provides a quantitative assessment of the damage performance of a material compared to statistical measurements of the damage threshold (the standard method thus far) [3,7] which are difficult to accurately determine due to the probabilistic nature of nanosecond damage initiation. The experiments involved the exposure of bulk material to individual pulses at a single wavelength at incremental fluences and to spatially and temporally overlapping 355- and 532-nm pulses at

various fluence combinations. The 355- and 532-nm pulses (having durations at FWHM of 4 ns and 2.5 ns, respectively) were aligned to co-propagate and focused by a 200-mm focal length cylindrical lens at the same location within the bulk of the material. A counter-propagating 632.8-nm He-Ne laser beam was focused into the tested volume by a 250-mm focal length cylindrical lens to illuminate any resulting damage sites. Images of the tested volumes were captured through the side of the sample using a microscope system equipped with a long-working-distance objective lens. The number of damage sites is counted over the region exposed to peak laser fluence (! 5%) having a height of ~340 μm and length of 5.8 mm. The $1/e^2$ of the 532-nm pulsed beam (~81 μm) was used in all experiments as the depth in calculating the volume (~0.16 mm^3 per tested site) and determining the PPD. Details on this experimental system can be found in Ref. 8. The samples were obtained from three conventionally grown crystal boules [1,2] and were uncoated, diamond-turn polished, and cut to 1×5×5 cm^3 in size.

Figure 1 shows the damage behavior of one of the samples under simultaneous exposure to combination of fluences at 5, 8, 12, 16, 20, and 24 J/cm^2 at 532 nm and 3, 5, 8, 10, 12, 15 and 20 J/cm^2 at 355 nm. The data are sorted into sets where the 532-nm fluence is kept constant while the 355-nm fluence is varied. The PPD at each combination of fluences was obtained from the average of four tested sites. Similar behaviors were observed in all samples studied although the PPD at a particular fluence combination varied between each material. These measurements demonstrate that the PPD resulting from simultaneous dual wavelength exposure is much larger than the total PPD resulting from separate exposures at each wavelength.

It is generally accepted that laser-induced damage in KDP/DKDP (or most other materials) is associated with the presence of an absorbing defect structure (damage precursor) [9-14]. A yet unknown physical property of the precursors (such as size) determines the fluence at which

damage is initiated. Independent of the absorption mechanism, it may be assumed that a fluence at one wavelength may be related to an effective fluence at the other wavelength that provides equivalent absorption of energy at the precursor. This assumption allows us to express the PPD under simultaneous exposure as

$$\begin{aligned} PPD(\phi_{532}, \phi_{355}) &= PPD(0, \phi_{355} + \phi_{355,eff}(\phi_{532})) \\ &\approx PPD(0, \phi_{355} + \gamma_{355/532} \cdot \phi_{532}) \end{aligned} \quad (1)$$

where $\gamma_{355/532}$ the ratio of the effective fluence at 355 nm over its corresponding fluence at 532 nm.

Applying Eq. (1) to our experimental results is equivalent to translating each PPD profile at constant 532-nm fluence by its corresponding $\phi_{355,eff}(\phi_{532})$ along the horizontal 355-nm fluence axis. To realize this approach, we first measured the 355-nm only ($\phi_{532} = 0$) profile over the full PPD range of the data and fit it to a power function. Figure 2 illustrates the best fit of all PPD profiles at constant 532-nm fluence (shown in Fig. 1) to the fit of the 355-nm only PPD profile. The results are presented on a semi-log scale to better depict the damage behavior at both high and low PPD values. This figure demonstrates that each profile overlaps to a section of the 355-nm only profile with a coefficient of determination (R^2) of 0.96 or greater.

Using this fitting procedure, the values of $\gamma_{355/532}$ for each profile at constant 532-nm fluence are extracted. The value of $\gamma_{355/532}$ as a function of the fluence at 532-nm is shown in Fig. 3. The data shown as solid circles are deduced from the measurements presented in Fig. 1. Data shown as open circles represent results from a second sample (from a different crystal boule) with a lower damage performance (higher PPD and lower damage threshold) illustrating an identical behavior within experimental error.

The mechanism that has been hypothesized and well developed for over a decade to account for damage initiation for pulses longer than about 50 ps assumes linear absorption by embedded nanoparticles [9-13]. Damage is associated with a particle having reached a critical temperature which results in localized mechanical and/or optical modification of the material [13]. According to this model, the total energy E absorbed by such a precursor from each harmonic can be written as:

$$E \propto \pi a^2 \cdot Q_{532} \cdot \phi_{532} + \pi a^2 \cdot Q_{355} \cdot \phi_{355} \tag{2}$$

where $\phi_{532,355}$ refers to fluences at 532 and 355 nm, the Q's refer to the absorption efficiencies of each precursor according to the Mie theory [15], and πa^2 is the cross sectional area of the precursor. From this expression, a fluence at 532 nm can be related to the effective fluence at 355 nm that provides equivalent absorption of energy at the precursor (as discussed above) that is determined by the ratio of the absorption efficiencies at each wavelength:

$$\phi_{355,eff} = \frac{Q_{532}}{Q_{355}} \cdot \phi_{532} \qquad or \qquad \gamma_{355/532} = \frac{Q_{532}}{Q_{355}}. \tag{3}$$

Mie theory predicts that the absorption efficiency of nanoparticles depends on their size and the wavelength of the absorbed light while absorption is introduced through the imaginary part of the index of refraction ($n = n_0 - ik$). Assuming that the larger particles will initiate damage at a lower laser fluence, the experimentally observed behavior of $\gamma_{355/532} = \frac{Q_{532}}{Q_{355}}$ as a function of the particle size (or equivalently as a function of laser fluence) can be predicted within the Mie theory formulation. We found that for imaginary parts of the index of refraction greater than 1, the results reproduced the same qualitative increase of the ratio with increasing fluence observed

in Fig. 3. However, in this range of values, $\frac{Q_{532}}{Q_{355}}$ was restricted to values greater than 1. This would indicate that the damage threshold fluence at 532 nm is lower than at 355 nm which is opposite to the damage characteristics observed at these wavelengths. Variation of this approach using different values of the real and imaginary part of the index of refraction at each wavelength does not alter this general behavior. Thus, the qualitative behavior predicted by the Mie theory in the linear absorption model does not adequately represent the experimental results shown in Fig. 3. This may suggest that a nonlinear absorption mechanism at the precursors is the mechanism leading to damage initiation (as suggested in Ref. 14) and governing our experimental observations. In this case, the change of $\gamma_{355/532}$ with fluence arises from the increasing contribution of the excited state absorption in the overall absorption coefficient. Within this model, a relative increase (compared to ground state only) of the ratio of the excited state absorption coefficient at 532 nm over that at 355 is suggested.

The correlation between the damage behaviors at 532 and 355 nm via the profile of $\gamma_{355/532}$ (shown in Fig. 3) offers a method to determine the expected PPD under any combination of fluences using the PPD profile at one wavelength only and without having to perform the extensive damage testing under simultaneous exposure. This is of practical importance towards simulating the damage behavior during harmonic conversion where multiple wavelengths are present. A part of the profile of $\gamma_{355/532}$ can also be directly obtained from the individual PPD profiles by calculating the ratio of the fluences at 355 nm and 532 nm that provide the same PPD. This process can be used for validation of only the upper part of the profile of $\gamma_{355/532}$ shown in Fig. 3 for any arbitrary DKDP sample since it is limited to using fluences above the damage threshold at each wavelength.

It is clear that, although this work provides insight into the fundamental mechanism governing damage initiation in KDP, additional experimental results probing complementary aspects of this mechanism are required in order to narrow down to a single mechanism. The results also suggest that the damage behavior of a material exposed to multiple wavelengths can be predicted from simple profiles that correlate the fluences at each excitation wavelength to corresponding effective fluences at a single wavelength. This greatly simplifies this complex problem by requiring the measurement of the damage characteristics at one wavelength only. The exact form of these profiles is governed by the damage initiation mechanism and the electronic structure of the damage precursors.

This work was performed under the auspices of the U.S. Department of Energy by the University of California, Lawrence Livermore National Laboratory under contract W-7405-Eng-48.

REFERENCES

[1]J. J. De Yoreo, A. K. Burnham, P. K. Whitman, Int. Mater. Rev. **47**, 113-152 (2002).

[2]N. P. Zaitseva, J. Atherton, R. Rozsa, L. Carman, I. Smolsky, M. Runkel, R. Ryon, and L. James, J. of Crystal Growth, **197**, 911 (1999).

[3]A. K. Burnham, M. Runkel, M. D. Feit, A.M. Rubenchik, R. L. Floyd, T. A. Land, W. J. Siekhaus, and R. A. Hawley-Fedder, Appl. Opt. **42**, 5483 (2003).

[4]R. M. Wood, Laser-Induced Damage of Optical materials, IOP Publishing LTD (2003).

[5]X. A. Shen, S. C. Jones, and P Braunlich, Phys. Rev. Lett. **62**, 2711 (1989).

[6]C. W. Carr and J. M. Auerbach, Opt. Lett. **31**, 595 (2006).

[7]H. Yoshida, T. Jitsuno, H. Fujita, M. Nakatsuka, M. Yoshimura, T. Sasaki, and K. Yoshida, Appl. Phys. B **70**, 195 (2000).

[8]P. DeMange, C. W. Carr, H. B. Radousky, and S. G. Demos, Rev. Sci. Instrum. **75**, 3298 (2004).

[9]R. W. Hopper, D. Uhlmann. Appl. Phys. **41**, 4023 (1970).

[10]S. I. Anisimov, V. A. Khokhlov, Instabilities in Laser-matter interaction, CRC Press Boca Raton, (1999).

[11]S. Papernov and A. W. Schmid, J. of Appl. Phys. **97**, 114906 (2005).

[12]F. Bonneau, P. Combis, J. L. Rullier, M. Commandre, A. During, J. Y. Natoli, M. J. Pellin, M. R. Savina, E. Cottancin, and M. Pellarin, Appl. Phys. Lett. **83**, 3855 (2003).

[13]M. D. Feit and A. M. Rubenchik, Proc. SPIE, **5273**, 74 (2004).

[14]C. W. Carr, H. B. Radousky, and S. G. Demos, Phys. Rev. Lett. **91**, 127402 (2003).

[15]H. C. van de Hulst, "Light Scattering by Small Particles", John Wiley (1957).

FIGURE CAPTIONS

FIG. 1. Plots of the PPD profiles at constant 532-nm fluences versus 355-nm fluence.

FIG. 2. Best fit of PPD profiles at constant fluence at 532 nm (after translation along 355-nm fluence axis) to the 355-nm only PPD profile (shown with ⭘).

FIG. 3. The fluence ratio, $\gamma_{355/532}$, relating fluences at each wavelength providing equivalent damage effects versus fluence at 532 nm for two different samples (open and solid data points).

Figure 1, DeMange et al.

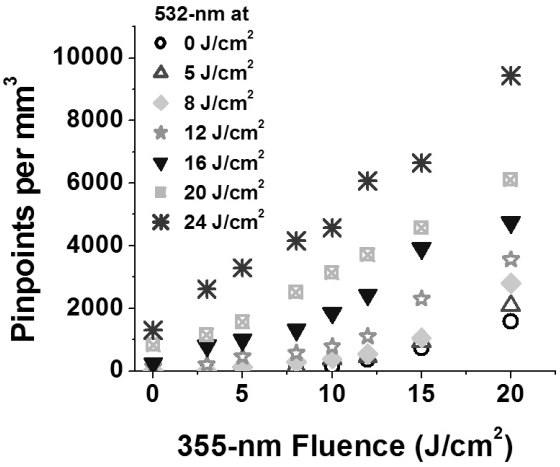

Figure 2, DeMange et al.

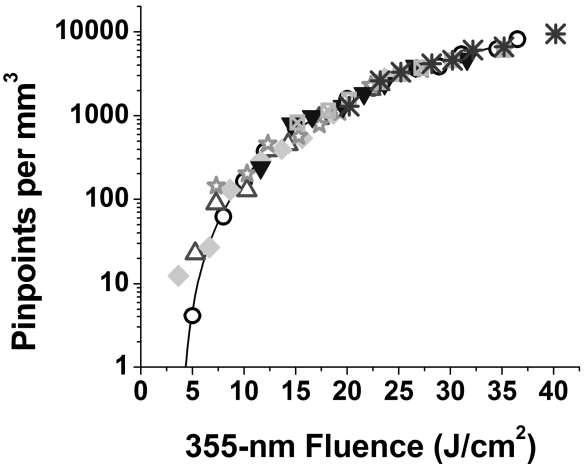

Figure 3, DeMange et al.